

A PI(3,4,5)P3-dependent allosteric switch controls antigenic variation in trypanosomes

Abdoulie O. Touray^{1,2}, Rishi Rajesh¹, Tony Isebe¹, Tamara Sternlieb¹, Mira Loock¹, Oksana Kutova¹, Igor Cestari^{1,2,*}

¹Institute of Parasitology, McGill University, Sainte-Anne-de-Bellevue, QC H9X 3V9, Canada

²Division of Experimental Medicine, Department of Medicine, McGill University, Montreal, QC, H4A 3J1, Canada

* Correspondence: igor.cestari@mcgill.ca

Abstract: African trypanosomes evade host immune clearance by antigenic variation, causing persistent infections in humans and animals. These parasites express a homogeneous surface coat of variant surface glycoproteins (VSGs). They transcribe one out of hundreds of VSG genes at a time from telomeric expression sites (ESs) and periodically change the VSG expressed by transcriptional switching or recombination. The mechanisms underlying the control of VSG switching and its developmental silencing remain elusive. We report that telomeric ES activation and silencing entail an on/off genetic switch controlled by a nuclear phosphoinositide signaling system. This system includes a nuclear phosphatidylinositol 5-phosphatase (PIP5Pase), its substrate PI(3,4,5)P3, and the repressor-activator protein 1 (RAP1). RAP1 binds to ES sequences flanking VSG genes via its DNA binding domains and represses VSG transcription. In contrast, PI(3,4,5)P3 binds to the N-terminus of RAP1 and controls its DNA binding activity. Transient inactivation of PIP5Pase results in the accumulation of nuclear PI(3,4,5)P3, which binds RAP1 and displaces it from ESs, activating transcription of silent ESs and VSG switching. The system is also required for the developmental silencing of VSG genes. The data provides a mechanism controlling reversible telomere silencing essential for the periodic switching in VSG expression and its developmental regulation.

Keywords: Trypanosomes, antigenic variation, repressor-activator protein 1 (RAP1), phosphoinositides, signaling.

Abbreviations: PI(3,4,5)P3, phosphatidylinositol-(3,4,5)-triphosphate; PIP5Pase, phosphatidylinositol phosphate 5-phosphatase; RAP1, repressor-activator protein 1; ES, expression site; VSG, variant surface glycoproteins.

34 Introduction

35 Antigenic variation is a strategy of immune evasion used by many pathogens to maintain persistent
 36 infections and entails changes in surface antigens to escape host immune clearance. The single-celled
 37 protozoa *Trypanosoma brucei* spp. circulate in the mammalian host bloodstream and periodically change
 38 their variant surface glycoprotein (VSG) coat to evade antibody clearance by antigenic variation (1). *T.*
 39 *brucei* have over 2,500 VSG genes and pseudogenes, primarily on subtelomeres, and ~20 telomeric
 40 expression sites (ESs), each containing a VSG gene (Fig 1A). Only one VSG gene is transcribed at a
 41 time from a telomeric ES. Antigenic variation occurs via transcriptional switching between ESs or VSG
 42 gene recombination within ESs (1). The active VSG gene is developmentally regulated, and its
 43 expression is silenced in parasites encountered in the tsetse fly vector, e.g., procyclics and epimastigotes.
 44 Epimastigotes develop into transmissible metacyclic trypomastigotes, which re-activate VSG gene
 45 expression before infecting mammals. The coordinated activation and silencing of telomeric ESs is
 46 essential for the periodic switch in VSG gene expression during antigenic variation and VSG
 47 developmental regulation; however, the mechanisms underlying the control of this process remain
 48 unknown.

49 The expressed VSG gene is transcribed by RNA polymerase I (RNAP I) from a compartment outside the
 50 nucleolus termed ES body (ESB) (2). Transcription initiates in all ESs but only elongates through one ES
 51 (hereafter called active ES), resulting in VSG monogenic expression. The silencing of ES VSG genes
 52 involves its proximity to telomeres (3, 4) and the telomere-associated factor repressor-activator protein 1
 53 (RAP1) (5). RAP1 is conserved among eukaryotes (5-8) and functions in telomere silencing (5, 8),
 54 telomere end protection (9-11), and non-telomeric gene regulation in mammals and yeast (8, 11).
 55 Histones and chromatin-modifying enzymes, such as histone methyltransferase and bromodomain
 56 proteins, also associate with ESs and contribute to their repression (12-15). In contrast, the active ES is
 57 depleted of nucleosomes (12) and enriched in proteins that facilitate its transcription, e.g., VSG
 58 exclusion (VEX) 1 and 2 and ES body 1 (ESB1), and processing of the highly abundant VSG mRNAs
 59 (16, 17).

60 The mechanisms underlying the initiation or control of VSG switching remain unknown. Antigenic
 61 variation was thought to occur stochastically (18) with the DNA break and repair machinery involved in
 62 VSG recombination (19-22). However, we showed that phosphoinositide signaling plays a role in the
 63 expression and switching of VSG genes (23, 24). This system entails the plasma membrane/cytosolic-
 64 localized phosphatidylinositol phosphate 5-kinase (PIP5K) and phospholipase C (PLC) (23), and the
 65 nuclear phosphatidylinositol phosphate 5-phosphatase (PIP5Pase). The PIP5Pase enzyme interacts with
 66 RAP1 (24, 25), and either protein knockdown results in the transcription of all ESs simultaneously (5,
 67 23, 24). RAP1 and PIP5Pase interact with other nuclear proteins, including nuclear lamina, nucleic acid
 68 binding proteins, and protein kinases and phosphatases (24). The involvement of phosphoinositide
 69 signaling in VSG expression and switching implied that signaling and regulatory processes have a role in
 70 antigenic variation linking cytosolic and nuclear proteins to control transcriptional and recombination
 71 mechanisms.

72 We report here that PIP5Pase, its substrate PI(3,4,5)P3, and its binding partner RAP1 form a genetic
 73 regulatory circuit that controls ES activation and repression. We show that RAP1 binds to silent

telomeric ESs sequences flanking the VSG genes, and the binding is essential for VSG transcriptional repression. This association is regulated by PI(3,4,5)P3, which binds to the N-terminus of RAP1, acting as an allosteric regulator controlling RAP1-ES interactions. The system depends on PIP5Pase catalytic activity, which dephosphorylates PI(3,4,5)P3 and prevents its binding to RAP1. Inactivation of PIP5Pase results in PI(3,4,5)P3 and RAP1 binding, which displaces RAP1 from ESs, leading to transcription and switching of VSGs in the population. Hence, PIP5Pase activity is required for RAP1 association with silent ESs and VSG gene transcriptional control. The regulatory system is essential for VSG developmental silencing, and temporal disruption of this nuclear signaling system results in VSG switching. The data provide a molecular mechanism by which ESs are periodically turned on and off during antigenic variation and parasite development.

Results

PIP5Pase activity controls VSG switching and developmental silencing

To investigate the role of PIP5Pase activity in VSG gene expression and switching, we performed gene expression analysis in *T. brucei* bloodstream forms that exclusively express a wildtype (WT) or a catalytic mutant D360A/N362A (Mut) PIP5Pase; the latter is unable to dephosphorylate PI(3,4,5)P3 (24). The exclusive expression cells have the endogenous PIP5Pase alleles replaced by drug-selectable markers, a tetracycline (tet)-regulatable PIP5Pase allele introduced in the silent rDNA spacer, and a V5-tagged WT or Mut PIP5Pase allele in the constitutively expressed tubulin loci (24). In the absence of tet, the cells exclusively express the WT or Mut PIP5Pase allele (24). We performed RNA-seq after 24h exclusive expression of the WT or Mut PIP5Pase with Oxford nanopore sequencing (~500 bp reads) to distinguish the VSG genes expressed. The expression of the Mut PIP5Pase resulted in 1,807 genes upregulated and 33 downregulated (Fig 1B, ≥ 2 -fold change, p -value ≤ 0.01 , Data S1). Notably, all silent ES VSG genes were upregulated (Fig 1B and C), consistent with their transcription. In contrast, there was a ~10-fold decrease in the active VSG (VSG2) and ESAG mRNAs (Fig 1B and C), implying decreased expression of the active ES (BES1) genes, perhaps resulting from competition among ESs for polymerase or factors required for their transcription. The remaining upregulated genes were primarily from silent subtelomeric arrays, largely VSG genes and pseudogenes (Fig 1B and D), indicating that PIP5Pase activity is also required for subtelomeric ES repression. Re-establishing expression of WT PIP5Pase for 60h after its 24h withdrawal restored VSG monogenic expression. However, analysis of this population by VSG-seq revealed the expression of several VSGs other than the initially expressed VSG2 indicating a switch in VSG expression (Fig 1E). Analysis of isolated clones after PIP5Pase knockdown confirmed VSG switching in 93 out of 94 (99%) of the analyzed clones (Fig 1F, Fig S1). The cells switched to express VSGs from silent ESs or subtelomeric regions, indicating switching by transcription or recombination mechanisms. In contrast, only a few VSGs were detected in cells expressing WT PIP5Pase by VSG-seq (Fig 1E). Moreover, no switching was detected in 118 isolated clones from cells expressing WT PIP5Pase (Fig F). The data imply that PIP5Pase activity can control the transcription and switching of VSGs.

The active VSG gene is expressed in bloodstream forms but silenced during parasite development to the insect stage procyclic forms. To determine whether PIP5Pase is required for VSG developmental

silencing, we generated procyclics conditional nulls expressing a tet-regulatable V5-tagged PIP5Pase (Fig S2). Immunofluorescence analysis showed that PIP5Pase-V5 localizes in the nucleus of procyclic forms (Fig S2), as in bloodstream forms (23). Western analysis showed that PIP5Pase-V5 proteins were eliminated 72h after knockdown (Fig 1G), and growth arrest was detected after five days of knockdown (Fig S2). Gene expression analysis showed a 5-15 log₂-fold upregulation of all ES VSG genes at 72h (Fig 1H) at a time when cells are viable and dividing. The data indicate that VSG switching and developmental silencing depend on PIP5Pase activity.

RAP1 bind to VSG flanking sequences in silent telomeric ESs

Because PIP5Pase and its substrate PI(3,4,5)P₃ interact with RAP1 (24), we postulated that VSG silencing might involve the regulation of RAP1's repressive function. RAP1 binds telomeric repeats (5), but it is unknown if it binds to ESs or other genomic sequences. We performed ChIP-seq with a cell line expressing an *in-situ* HA-tagged RAP1 and nanopore sequencing (~500 bp reads). We found that RAP1-HA binds primarily to silent ESs at the 70 bp and telomeric repeats, which are sequences flanking VSG genes in bloodstream-form ESs (Fig 2A-B, E and Fig S3; *p*-values < 10⁻⁴). There was also a slight enrichment of RAP1-HA in the 50 bp repeat sequences preceding the ES promoters (Fig 2A and Fig S3; *p*-values < 10⁻⁴). However, RAP1-HA did not bind to genes, including VSG genes or pseudogenes in the ESs or subtelomeric regions (Fig 2A-B, F). Notably, analysis of uniquely mapped reads showed that RAP1-HA was depleted from the active ES (Fig 2C-D), consistent with RAP1 having a repressive function. The RAP1-HA bound sequences are rich in TAAs and GTs, including the 70 bp (TTA)₇(GT/A)₉ and telomeric (TTAGGG)_n repeats (Fig 2A). RAP1-HA was also bound to metacyclic ESs at AT/GC-rich or (TAACCC)_n repeat sequences near VSG genes (Fig 2E, *p*-values < 10⁻⁴, Fig S4). RAP1-HA also bound sparsely to subtelomeric regions, including centromeres (Fig 2F, *p*-values < 10⁻⁴), which are AT-rich in trypanosomes (26), and some binding sites overlapped with the centromeric protein kinetoplastid kinetochore 2 (KKT2) (27). Other poorly enriched RAP1-HA peaks in the subtelomeric regions reflect residual ES sequences from recombination (Fig 2F). Hence, RAP1-HA binds primarily to telomeric and 70 bp repeats within silent ESs. The 70 bp repeats are ES-specific sites for RAP1 binding near silent VSG genes.

To confirm RAP1 binding to ES sequences, we expressed and purified from *E. coli* recombinant 6xHis-tagged *T. brucei* RAP1 (rRAP1) (Fig 3A-B). We performed electrophoretic mobility shift assays (EMSA) using rRAP1 and biotinylated telomeric repeats, 70 bp repeat, or a scrambled telomeric repeat sequence as a control. rRAP1 bound to telomeric and 70 bp repeats but not to the scramble DNA sequence (Fig 3C). We obtained similar results by microscale thermophoresis (MST) kinetics using rRAP1 and Cy5-labelled DNA sequences (Fig 3D, Fig S5), with a K_d of 24.1 and 10 nM for telomeric and 70 bp repeats, respectively (Table 1). RAP1 has two DNA binding domains, a central Myb (position E426-Q500) and a C-terminal Myb-like (MybL, position E639-R761) domain (Fig 3A), and a divergent BRCT domain (S198-P385) (5), which is involved in RAP1 self-interaction (28) and perhaps other protein interactions (23, 24). To identify which RAP1 domain mediates DNA interactions, we performed EMSA with rRAP1¹⁻³⁰⁰ (aa positions in superscript), rRAP1³⁰¹⁻⁵⁶⁰, and rRAP1⁵⁶¹⁻⁸⁵⁵, the last two fragments encompass the Myb and MybL domains, respectively (Fig 3A-B). Both rRAP1³⁰¹⁻⁵⁶⁰ and

rRAP1⁵⁶¹⁻⁸⁵⁵ proteins bound to telomeric or 70 bp repeats (Fig 3E-F, Fig S5), but no DNA binding was detected with the N-terminal rRAP1¹⁻³⁰⁰ (Fig 3G). Because all proteins were His-tagged and no binding was detected with rRAP1¹⁻³⁰⁰, unspecific DNA binding by the His-tag is ruled out. Notably, disruption of the MybL domain sequence did not eliminate RAP1-telomere binding *in vivo* (29). Concurring, our data imply that the Myb domain can compensate for the MybL disruption and show that both Myb and MybL can independently and directly bind to 70 bp and telomeric repeats.

PIP5Pase activity controls PI(3,4,5)P3 binding to the N-terminus of RAP1

We found in the N-terminus of RAP1 a villin headpiece (VHP) domain (Fig 3A, position Y59 to F94, *e*-value < 10⁻⁴), which is typically present in Villin proteins and binds phosphoinositides (30). *T. brucei* RAP1 VHP domain is conserved (~27% aa identity) with other VHPs in Villin proteins forming a three helices fold over a hydrophobic core (31, 32) (Fig 4A), which is essential for phosphoinositide binding (30). We performed binding assays with rRAP1 and biotinylated phosphoinositides (25) and confirmed that rRAP1 binds specifically to PI(3,4,5)P3 (Fig S5) (24). Moreover, we found that rRAP1¹⁻³⁰⁰ binds to PI(3,4,5)P3 (Fig 4B), but not other phosphoinositides or inositol phosphates tested (Fig 4C) and the binding was competed by a molar excess of unlabelled PI(3,4,5)P3 (Fig 4D). However, no PI(3,4,5)P3 binding was detected with rRAP1³⁰¹⁻⁵⁶⁰ or rRAP1⁵⁶¹⁻⁸⁵⁵ proteins, indicating that RAP1 binds to PI(3,4,5)P3 via its N-terminus containing the VHP domain. Moreover, binding kinetics by differential scanning fluorescence with unlabelled phosphoinositides showed that rRAP1 binds to PI(3,4,5)P3 with a K_d of 19.7 μM (Fig 4E, Table 1). To determine if RAP1 binds to PI(3,4,5)P3 *in vivo*, we *in-situ* HA-tagged RAP1 in cells that express the WT or Mut PIP5Pase and analyzed PI(3,4,5)P3 levels associated with immunoprecipitated RAP1-HA. There were ~100-fold more PI(3,4,5)P3 associated with RAP1-HA in cells expressing the Mut than the WT PIP5Pase (Fig 4F, Fig S6). In contrast, there was a mild but not significant difference in the total cellular PI(3,4,5)P3 levels comparing cells expressing WT versus Mut PIP5Pase (Fig 4F), implying that PIP5Pase activity controls a localized pool of PI(3,4,5)P3 in the nucleus available for RAP1 binding. Hence, RAP1 binds specifically to PI(3,4,5)P3 via its N-terminus in a PIP5Pase activity-dependent fashion.

PI(3,4,5)P3 is an allosteric regulator of RAP1 and controls telomeric ES repression

Because RAP1 binds to PI(3,4,5)P3 via its N-terminus and to ESs via its central and C-terminus Myb and Myb-L domains, we posited that PI(3,4,5)P3 binds to RAP1 and controls its association with ESs. We performed EMSA binding assays and found that PI(3,4,5)P3 inhibited rRAP1 binding to telomeric repeats in a dose-dependent fashion, but no inhibition was detected with PI(4,5)P2 (Fig 5A-B). Similar PI(3,4,5)P3 binding inhibition of RAP1 was observed for 70 bp repeats (Fig 5B). Moreover, MST binding kinetics with 30 μM of PI(3,4,5)P3 increased rRAP1 K_d to telomeric and 70 bp repeats in ~6.5-fold and ~18.5-fold, respectively (Fig 5C, Table 1). Notably, PI(3,4,5)P3 did not affect rRAP1³⁰¹⁻⁵⁶⁰ or rRAP1⁵⁶¹⁻⁸⁵⁵ binding to telomeric or 70 bp repeats (Fig S5), implying that PI(3,4,5)P3 does not compete with Myb or MybL domains direct binding to DNA. PI(3,4,5)P3 inhibition of RAP1-DNA binding might

192 be due to its association with RAP1 N-terminus causing conformational changes that affect Myb and
193 MybL domains association with DNA.

194 Our data suggest a model in which PI(3,4,5)P3 levels control RAP1 binding to ESs and thus silencing
195 and activation of VSG genes. To evaluate this model, we performed ChIP-seq with RAP1-HA in cells
196 that exclusively express WT or Mut PIP5Pase. The Mut PIP5Pase expression results in local PI(3,4,5)P3
197 available for RAP1 binding (Fig 4F), whereas WT PIP5Pase dephosphorylates PI(3,4,5)P3 into
198 PI(3,4)P2, which cannot bind RAP1 (24). The expression of Mut PIP5Pase abolished RAP1-HA binding
199 to 70 bp, 50 bp, and telomeric repeats in all bloodstream and metacyclic ESs (Fig 5D-G). Notably, the
200 decreased RAP1-HA binding to ESs correlates with increased expression of VSGs and ESAG genes (Fig
201 5D-E, RNAseq), indicating that PIP5Pase controls RAP1 binding to ESs and thus VSG gene expression.
202 The expression of Mut PIP5Pase also removed RAP1-HA peaks in subtelomeric regions (Fig 2F), which
203 might impact subtelomeric chromatin organization and thus VSG expression and recombination (Fig 1D-
204 F). We showed that RAP1 interacts with PIP5Pase within a 0.9 MDa complex, and this association is
205 stable in cells expressing the Mut PIP5Pase (24). Hence, RAP1 dissociation from ESs is unlikely the
206 result of PIP5Pase mutations affecting the complex integrity. Our data indicate that PIP5Pase activity
207 regulates RAP1 binding to DNA via PI(3,4,5)P3, thus controlling the reversible silencing of telomeric
208 VSG genes.

209

210 Discussion

211 We found that the reversible silencing of telomeric VSG genes in *T. brucei* is controlled by a
212 phosphoinositide regulatory system. The system operates via PI(3,4,5)P3 regulation of RAP1-DNA
213 binding and is controlled by PIP5Pase enzymatic activity. The system functions as an on/off genetic
214 switch to control telomeric ES activation and silencing and provides a mechanism to control the periodic
215 switching of VSG genes during antigenic variation and VSG developmental silencing. The regulation
216 requires PIP5Pase activity for continuous ES repression via dephosphorylation of PI(3,4,5)P3. PIP5Pase
217 temporary inactivation results in the accumulation of PI(3,4,5)P3 bound to the RAP1 N-terminus. This
218 binding displaces RAP1 Myb and MybL domains from DNA, likely due to RAP1 conformational
219 changes, allowing polymerase elongation through the VSG gene. PI(3,4,5)P3 acts as a typical allosteric
220 regulator controlling RAP1-DNA interactions and, thus, VSG transcriptional repression.

221 Our data indicate that regulation of PIP5Pase activity and PI(3,4,5)P3 levels play a role in VSG
222 switching. Other phosphoinositide enzymes such as PIP5K or PLC, which act on PI(3,4,5)P3 precursors,
223 also affect VSG expression and switching (23), arguing that this system is part of a cell-wide signaling
224 network and includes the transcriptional and recombination machinery. The finding of RAP1 binding at
225 subtelomeric regions, including at centromeres, requires further validation. Nevertheless, it suggests a
226 role for RAP1 repressing subtelomeric chromatin. Chromatin conformational capture analysis showed
227 that subtelomeric regions and centromeres have a high frequency of interactions forming the boundaries
228 of genome compartments in *T. brucei* (13). Disrupting PIP5Pase activity affects RAP1 association with
229 those regions and, thus, might impact long-range chromatin interactions. This organization may explain
230 RAP1's role in VSG recombinational switching (33) and the transcription of subtelomeric VSGs upon
231 PIP5Pase mutation, RAP1 (29) or NUP1 knockdowns (34).

RAP1 and PIP5Pase interact and localize near the nuclear periphery (23, 24). RAP1 also associates with NUP1 (24), which knockdown derepresses silent VSG genes (34). PI(3,4,5)P3 and other phosphoinositides are synthesized in the endoplasmic reticulum (ER) and Golgi (35, 36) and distributed to organelles, including the nuclear membrane (23, 36). The scenario suggests a model in which RAP1 associates with silent telomeric ESs and lamina proteins at the nuclear periphery (13, 23, 34), where regulation of silencing and activation might occur. The compartmentalization of silent ESs near the nuclear lamina may prevent the association of factors required for ES transcription, including chromatin-associated proteins and RNA processing factors. In contrast, the active ES is depleted of RAP1, a process that might involve ES mRNAs competition for RAP1 binding to ES DNA (37), and it is enriched in proteins that facilitate transcription, including VEX2 and ESB1 (17, 38). Furthermore, the active ES localizes in a compartment that favours efficient processing of VSG mRNAs (39, 40). Hence, the active and silent ESs seem to occupy distinct subnuclear compartments and have specific associated proteins. Within this model, VSG switching may entail the inactivation of PIP5Pase, leading to reorganization of silent ES chromatin, e.g., RAP1 removal from ESs, ESs relocation away from the nuclear lamina, and perhaps changes in ES three-dimensional organization (Fig S7). Once RAP1 is dissociated from ESs, other factors, such as ESB1 and VEX2, may associate with the silent ESs to initiate transcription. Although the requirements for establishing VSG monogenic expression are unknown, it may entail the successful association of factors with ESs for their transcription or recruitment to the ESB (2, 39).

How the phosphoinositide signaling system is initiated to control VSG switching is unknown, but our data imply that antigenic variation is not exclusively stochastic. Moreover, it implies that trypanosomes evolved a sophisticated mechanism to regulate antigenic variation that entails genetic and signaling processes, and such processes may be conserved in other pathogens that rely on antigenic variation for infection, e.g., *Plasmodium* and *Giardia*, broadening opportunities for drug discovery. The allosteric regulation of RAP1 by PI(3,4,5)P3 denotes a mechanism for phosphoinositide regulation of telomere silencing. Given that telomere silencing is conserved and dependent on RAP1 in most eukaryotes, this regulatory system may be present in other eukaryotes.

Materials and Methods

Cell culture, cell lines, and growth curves

T. brucei bloodstream forms (BF) single marker 427 conditional null (CN) and V5- or HA-tagged cell lines were generated and maintained in HMI-9 at 37°C with 5% CO₂ as described (23). Cell lines that exclusively express wildtype (WT) or mutant D360A/N360A (Mut) PIP5Pase gene (Tb927.11.6270) were generated as previously described (24). *T. brucei* 29.13 were maintained in SDM-79 medium supplemented with 10% FBS, G418 (2.5 µg/mL), and hygromycin (50 µg/mL) at 27°C. To generate *T. brucei* procyclic forms (PF) CN PIP5Pase, PF 29.13 was transfected with a V5-tagged PIP5Pase gene cloned into pLEW100-3V5 (23). The plasmid was integrated into the rRNA silent spacer, and transgenic cells were selected by resistance to phleomycin (5 µg/mL). The PIP5Pase endogenous alleles were then sequentially replaced by homologous recombination with PCR constructs containing about 500 bp of the PIP5Pase 5'UTR and 3'UTR flanking a puromycin or blasticidin drug resistance gene (23). The

8CRISPR/Cas9 ribonucleoprotein complex was used to cut the second endogenous allele and increase homologous recombination rates. Guides targeting 5' and 3' regions (see primer sequences in Table S2) of the PIP5Pase coding sequence were produced by in vitro transcription with T7 polymerase (Promega), and co-transfected with recombinant saCas9 Nuclease NLS Protein (Applied Biological Materials Inc.), and a PCR-based puromycin resistance construct containing 5'- and 3'-UTRs of the targeted gene. Note that this procedure increased the efficiency of recombination by about 20 times. Cumulative growth curves were performed by diluting *T. brucei* PFs to 2×10^6 parasites/mL in the absence or presence of tetracycline (tet, 0.5 μ g/mL). The culture growth was counted every two days using a Coulter Counter (Beckman Coulter) for twelve days.

Immunofluorescence and Western blotting

Immunofluorescence: Immunofluorescence was done using *T. brucei* PF PIP5Pase CN, which expresses V5-tagged WT PIP5Pase in the presence of 0.1 μ g/mL of tet. Mid-log growth phase parasites were washed three times in PBS with 6 mM glucose (PBS-G) for 10 minutes (min). Then, 2.0×10^6 cells were fixed in 2% paraformaldehyde in PBS for 10 min at room temperature (RT) onto poly L-lysine treated 12 mm glass coverslips (Fisher Scientific). The coverslips were washed three times in PBS, and cells permeabilized in 0.2% Nonidet P-40 in PBS for 10 min. Cells were washed five times in PBS, and then blocked for 1 hour (h) in 10% nonfat dry milk in PBS. After, cells were incubated in α -V5 mouse monoclonal antibodies (mAb) (Thermo Life Technologies) diluted 1:500 in 1% milk in PBS for 2 h at RT. The cells were washed five times in PBS and incubated in goat α -mouse IgG (H+L) Alexa Fluor (Invitrogen) 1:1,000 in 1% milk in PBS for 2 h at RT. Cells were washed five times in PBS and stained in 10 μ g/mL of 4',6-diamidino-2-phenylindole (DAPI) diluted in PBS for 15 min at RT. Cells were washed four times in PBS, twice in water, and then mounted onto microscope glass slides (Fisher Scientific) using a mounting medium (Southern Biotech). Cells' images were acquired using a Nikon E800 Upright fluorescence microscope (Nikon). **Western blotting:** Western analyses were performed as previously described (25). Briefly, cleared lysates of *T. brucei* PFs were prepared in 1% Triton X-100 in PBS with 1X protease inhibitor cocktail (Bio-Vision) and mixed in 4X Laemmli buffer (Bio-Rad) with 710 mM β -mercaptoethanol and heated for 5 min at 95°C. Proteins were resolved in 10% SDS/PAGE and transferred to nitrocellulose membranes (Sigma Aldrich). Membranes were probed for 2 h at RT (or overnight at 4°C) with mAb α -V5 (BioShop Canada Inc.) 1:2,500 in 6% milk in PBS 0.05% Tween (PBS-T). Membranes were incubated in 1:5,000 goat anti-mouse IgG (H+L)-HRP (Bio-Rad) in 6% milk in PBS-T, washed in PBS-T, and developed by chemiluminescence using Supersignal West Pico Chemiluminescent Substrate (Thermo scientific). Images were acquired on a ChemiDoc MP imaging system (Bio-Rad). Membranes were stripped in 125 mM glycine, pH 2.0, and 1% SDS for 30 min, washed in PBS-T, and re-probed with mAb anti-mitochondrial heat shock protein (HSP) 70 of *T. brucei* (gift from Ken Stuart, Center for Global Infectious Diseases Research, Seattle Children's) 1:25 in 3% milk in PBS-T, followed by 1:5,000 goat anti-mouse IgG (H+L)-HRP (Bio-Rad) in 3% milk in PBS-T and developed as described above.

Protein expression and purification

The *T. brucei* RAP1 (Tb927.11.370) recombinant protein was expressed and purified as described before (24). The RAP1 fragments rRAP1¹⁻³⁰⁰ (aa 1-300), rRAP1³⁰¹⁻⁵⁶⁰ (aa 301-560), or rRAP1⁵⁶¹⁻⁸⁵⁵ (aa 561-

855) were amplified by PCR (see Table S2 for primers) from the *T. brucei* 427 genome and cloned into the pET-29a(+) vector (Novagen) using *NdeI* and *XhoI* restriction sites for the expression of proteins with a C-terminal 6xHis tag. Proteins were expressed and purified from 2 to 4 liters of *Escherichia coli* NiCo21(DE3) (New England Biolabs) as previously described (24). Briefly, lysates were sonicated in PBS supplemented with 5 mM dithiothreitol (DTT), 0.2 mg/mL lysozyme, 0.05% NP-40, 10% glycerol, and 1 mM PMSF. For rRAP1¹⁻³⁰⁰, this buffer was supplemented with 7 M of urea (Fisher Scientific). After sonication, His-tagged proteins in the cleared lysate were purified using Profinity™ IMAC Nickel Charged Resin (Bio-Rad) and eluted in 50 mM sodium phosphate buffer with 300 mM NaCl pH 8 and 300 mM imidazole (Fischer Scientific). Eluted proteins were dialyzed overnight at 4°C in binding buffer (25 mM HEPES, 150 mM NaCl, 10% glycerol, pH 7.5).

Phosphoinositide binding assays

Phosphoinositide binding assays were performed as previously described (20). Briefly, 1 µg of His-tagged recombinant protein (rRAP1, rRAP1¹⁻³⁰⁰, rRAP1³⁰¹⁻⁵⁶⁰, or rRAP1⁵⁶¹⁻⁸⁵⁵) was incubated with 1 µM of biotin-conjugated dioctanoylglycerol (diC8) PI(3,4,5)P3, diC8 PI(4,5)P2, InsP(1,4,5)P3 or InsP(1,3,4,5)P4 (Echelon Biosciences) rotating at RT for 1 h. Afterward, magnetic streptavidin beads (Sigma Aldrich) (previously blocked overnight at 4°C with 3% BSA in PBS) were added and incubated at 4°C for 1 h rotating. Using a magnetic stand, the mix was washed 5-6 times in 25 mM HEPES pH 7.5, 300 mM NaCl, 0.2% NP-40 and 0.1% Tween 20, and then eluted in 50 µL of 2x Laemmli buffer supplemented with 710 mM β-mercaptoethanol. Samples were boiled at 95°C for 5 min. Samples were resolved in 10% SDS-PAGE, transferred onto a nitrocellulose membrane (Sigma Aldrich), and probed with □-His mAb (Thermo Scientific) diluted 1:1,000 in 6% milk in PBS-T followed by α-mouse IgG HRP (Bio-Rad) diluted 1:5,000 in 6% milk in PBS-T. Membranes developed as indicated above.

Electrophoretic mobility shift assays

Synthetic single-stranded 5'-biotin-conjugated DNA sequences (Table S2) of telomeric repeats (TTAGGG)₁₀, 70 bp repeats (one repeat), and scrambled DNA (derived from telomeric repeats) were annealed (1:1 v/v, 10 µM) to reverse complementary unlabeled sequences (Table S2) (Integrated DNA Technologies) in a thermocycler by incubation at 95°C for 10 min, 94°C for 50 seconds, and a gradual decrease of 1°C every 50 seconds for 72 cycles in 200 mM Tris-HCl pH 7.4, 20 mM MgCl₂, 500 mM NaCl. 100 nM of annealed DNA were mixed with 1 µg of recombinant protein, and 2 mg/mL yeast tRNA (Life Technologies) in 20 mM HEPES, 40 mM KCl, 10 mM MgCl₂, 10 mM CaCl₂, and 0.2% NP-40, and incubated on a thermomixer (Eppendorf) at 37°C for 1 h. Then, 10 µL of the reaction was resolved on a 6% native gel (6% acrylamide in 200 mM Tris, 12.5 mM ethylenediaminetetraacetic acid (EDTA), pH 7.8 adjusted with acetic acid) at 100 V in 0.5 X TAE buffer (40 mM Tris, 20 mM acetic acid, and 1 mM EDTA). DNAs were transferred onto a nylon membrane (Life Technologies) at 100 V for 30 min in 0.5x TAE. The membrane was blocked for 1 h at RT with nucleic acid detection blocking buffer (Life Technologies), then probed for 1 h at RT with streptavidin-HRP 1:5,000 (Genescript) diluted in PBS 3% BSA. The membrane was washed in PBS-T and developed using Supersignal West Pico Chemiluminescent Substrate (Thermo Fisher Scientific). Images were acquired with a ChemiDoc MP imaging system (Bio-Rad).

Microscale thermophoresis binding kinetics

Binding assays were performed using synthetic single-stranded 5'-Cy5 conjugated DNA sequences of telomeric repeats (TTAGGG)₁₀, 70 bp repeats (one repeat), or scrambled DNA (derived from telomeric repeats) (see Table S2 for sequences). Sequences were annealed (1:1 v/v, 10 μ M) to reverse complementary unlabeled sequences (Table S2, all sequences synthesized by Integrated DNA Technologies) in a thermocycler by incubation at 95°C for 10 min, 94°C for 50 seconds, and a gradual decrease of 1°C every 50 seconds for 72 cycles in 200 mM Tris-HCl pH 7.4, 20 mM MgCl₂, 500 mM NaCl. Then, 1 μ M rRAP1 was diluted in 16 two-fold serial dilutions in 250 mM HEPES pH 7.4, 25 mM MgCl₂, 500 mM NaCl, and 0.25% (v/v) N P-40 and incubated with 20 nM telomeric or 70 bp repeats for 2 h at 37 °C, gently shaking. Afterward, samples were centrifuged at 2,000 xg for 5 min, loaded into Monolith™ capillary tubes (NanoTemper Technologies), and analyzed using the Monolith NT.115 MicroScale Thermophoresis instrument with MO.Control software (NanoTemper Technologies). For binding assays in the presence of phosphatidylinositol phosphates (PIPs), the binding reaction was prepared as above but in the presence of 30 μ M of diC8 PI(3,4,5)P₃ or diC8 PI(4,5)P₂. Four to six replicates were performed and presented as mean \pm standard deviation. Data were analyzed using MO.Affinity Analysis (NanoTemper Technologies).

Differential Scanning Fluorimetry

T. brucei rRAP1 at 10 μ M was incubated with 10 mM SYPRO Orange dye (ThermoFisher Scientific), filtered before use with a 0.22 μ m sterile filter (Fisher scientific), in 15 mM HEPES, 150 mM NaCl, pH 7.0, and 10, 20, 30, or 40 μ M of diC8 PI(3,4,5)P₃, diC8 PI(4,5)P₂, or no PIPs in 96-well microplates (Life Technologies). The plate was sealed with MicroAmp® Optical Adhesive Film (Life Technologies), and the reaction mixture was placed on ice for 1 h. Afterward, 20 μ L of the reaction was added to a differential scanning fluorimetry plate (Life Technologies) and run using the Applied Biosystems StepOnePlus instrument (ThermoFisher Scientific) according to the manufacturer's instructions. Briefly, samples were run using continuous ramp mode with two thermal profiles: Step 1 at 25°C for 2 min and step 2 at 99°C for 2 min, with a ramp rate of 100% at step 1 and 1% at step 2. Experiments were performed in triplicate and presented as mean \pm standard deviation. Data analysis was performed using the DSFworld (<https://gestwickilab.shinyapps.io/dsfworld/>) platform, and melting temperatures were calculated as the midpoint of the resulting fluorescence versus temperature curve.

RNA-seq

Poly-A enriched RNAs were extracted from 1.0×10^8 *T. brucei* BFs CN PIP5Pase exclusively expressing V5-tagged PIP5Pase WT or mutant D360A/N362A for 24 h using the magnetic mRNA isolation kit (New England Biolabs) according to manufacturer's instructions. The isolated mRNA samples were used to synthesize cDNA using ProtoScript II Reverse Transcriptase (New England Biolabs) according to the manufacturer's instructions. cDNA samples were purified using Totalpure NGS mag-bind (Omega-BioTek) at a 1.0x ratio (beads to cDNA volume). cDNA samples were eluted in 55 μ L of water, then fragmented to a size range of 300bp – 1kb (average 700 bp) using an M220 Focused-ultrasonicator (Covaris) with 75 peak incidence power, 10% duty factor, and 200 cycles per burst for 35 seconds at 20 °C. The fragmented cDNAs were then used for RNA-seq library preparation for Oxford nanopore sequencing (indicated below). Fifty fmol of barcoded libraries were sequenced in a MinION (Oxford

398 Nanopore Technologies) using an FLO-MIN106 flow cell (Oxford Nanopore Technologies). Three
399 biological replicates were performed.

400

401 ChIP-seq

402 ChIP-seq was performed with *T. brucei* BF₃ CN PIP5Pase expressing endogenously HA-tagged RAP1
403 and exclusively expressing V5-tagged PIP5Pase WT or mutant D360A/N362A. Cells were grown for
404 24h in the absence of tet, which results in the exclusive expression of WT or mutant PIP5Pase, in HMI-9
405 media supplemented with 10% FBS, 2 µg/mL of G418, 2.5 µg/mL of phleomycin, 0.1 µg/mL of
406 puromycin, and 25 µg/mL of nourseothricin. A total of 3.0x10⁸ cells at mid-log growth were fixed in 1%
407 paraformaldehyde at 4°C for 10 min, then quenched for 10 min in 140 mM glycine. Fixed cells were
408 spun down at 2000 xg for 10 min, washed twice in PBS, and processed for ChIP using truChIP
409 Chromatin Shearing Kit with Formaldehyde (Covaris) according to the manufacturer's instructions. DNA
410 was sheared to a size range of 0.5-1.5 kb (average 700 bp) using an M220 Focused-ultrasonicator
411 (Covaris) with 75 peak incidence power, 5% duty factor, and 200 cycles per burst for 7 min at 7°C. ChIP
412 was performed with a total of 15 µg of sonicated chromatin and 10 µg of Mab anti-V5 (BioShop Canada
413 Inc.). The antibodies were cross-linked to Protein G Mag Sepharose Xtra (GE Healthcare) according to
414 the manufacturer's instructions before immunoprecipitations. Antibody eluted chromatin was incubated
415 with 20 units of Proteinase K (Thermo Fisher Scientific) and reverse cross-linked at 65°C overnight,
416 followed by DNA extraction by phenol:chloroform:isoamyl alcohol (25:24:1, ThermoFisher Scientific)
417 and isopropanol (v/v) precipitation. Samples were resuspended in water, and the DNA was selected for
418 fragments above 300 bp using Totalpure NGS mag-bind (Omega-BioTek) at 0.85x ratio (beads to DNA
419 volume). The DNA was eluted in water and used to prepare Oxford nanopore DNA sequencing libraries
420 (indicated below). Fifty fmol of barcoded libraries was sequenced in a MinION (Oxford Nanopore
421 Technologies) using an FLO-MIN106 flow cell (Oxford Nanopore Technologies). Three biological
422 replicates were performed.

423

424 VSG-seq

425 *T. brucei* BF₃ PIP5Pase CN cell lines exclusively expressing V5-tagged PIP5Pase WT or mutant
426 D360A/N362A were seeded at 1.0x10³ parasites/mL in 50 mL of HMI-9 media supplemented with 10%
427 FBS, 2 µg/mL of G418, 2.5 µg/mL of phleomycin, and grown for 24 h in the absence of tet, which
428 results in the exclusive expression of WT or PIP5Pase mutant. Then, tet (0.5 µg/mL) was added to Mut
429 PIP5Pase cells to rescue WT PIP5Pase expression, and cells were grown for an additional 60 h at 37°C
430 and 5% CO₂ until they reached a concentration of 1.0x10⁶ parasites/mL. RNA was then isolated using
431 Trizol (Sigma-Aldrich) according to the manufacturer's instructions. cDNA was synthesized using
432 random primers with 5x Protoscript II Reverse Transcriptase (New England BioLabs Ltd). cDNA was
433 amplified using the VSG Splice Leader and SP6-VSG14mer primers (41) (Table S2) with denaturing at
434 94°C for 3 min, followed by 22 cycles of 94°C for 1 min, 42°C for 1 min, and 72°C for 2 min (41).
435 Amplified fragments were purified using 0.55x beads/sample ratio with Mag-Bind® TotalPure NGS
436 (Omega Bio-Tek). Amplicons were prepared for Oxford Nanopore sequencing using the ligation
437 sequencing kit SQK-LSK110 (Oxford Nanopore Technologies) and PCR Barcoding Expansion kit

(EXP-PBC001) according to the manufacturer's instructions (described below). Five fmol pooled barcoded libraries were sequenced in a MinION using a Flongle FLO-FLG001 flow cell (Oxford Nanopore Technologies). Experiments were performed in three biological replicates.

Clonal-VSG-seq

T. brucei BFs PIP5Pase CN cell lines seeded at 1.0×10^4 parasites/mL in 10 mL of HMI-9 media supplemented with 10% FBS and 2 μ g/mL of G418 and 2.5 μ g/mL of phleomycin in the absence of tet (tet -) for PIP5Pase knockdown, or in the presence of tet (tet +, 0.5 μ g/mL) for PIP5Pase expression. After 24 h, tet (0.5 μ g/mL) was added to the tet - cells to restore PIP5Pase expression and cells were cloned by limited dilution. Briefly, the cells were diluted to a concentration of 1 parasite/300 μ L and grown in 200 μ L of media in 96-well culture plates (Thermo Scientific Inc.) and grown for 5-7 days at 37°C and 5% CO₂. Clones were collected from the plates and transferred to 24 well culture plates (Bio Basic Inc.) containing 2 mL of HMI-9 media with 10% FBS, 2 μ g/mL of G418, 2.5 μ g/mL of phleomycin, and 0.5 μ g/mL of tet for 24 h to reach 1.0×10^6 parasites/mL. Afterward, cells were harvested by centrifugation at 2,000 xg, and pellets were collected for RNA extraction using the 96 Well Plate Bacterial Total RNA Miniprep Super Kit (Bio Basic Inc.) according to the manufacturer's instructions. cDNA was synthesized from extracted RNA samples using M-MuLV reverse transcriptase kit (New England Biolabs Ltd) based on the manufacturer's instructions and using customized primers splice leader (SL_F) and VSG barcoded primers (BCA_Rd_3'AllVSGs 1 to 96) (see Table S2 for primer sequences). The forward SL F primer is complementary to the splice leader sequence and has an Oxford nanopore barcode adapter sequence. The reverse primer contains a sequence complementary to the 3'-region conserved among VSG genes, a unique 6 random nucleotide barcode sequence, and an Oxford nanopore barcode adapter sequence for library preparation. The synthesized cDNAs were pooled in a 1.5 mL Eppendorf tube and amplified using the Oxford nanopore library barcoding primers (PCR Barcoding Expansion kit EXP-PBC001, Oxford Nanopore Technologies) with denaturing at 95° for 3 min, followed by 22 cycles of 95°C for 30 sec, 60°C for 30 sec, and 72°C for 2.30 min. Amplified fragments were purified using 0.55x beads/sample ratio NucleoMag® NGS magnetic beads (Takara Bio). Amplicons were prepared for Oxford Nanopore sequencing using the ligation sequencing kit SQK-LSK110 (Oxford Nanopore Technologies) according to the manufacturer's instructions (details described below). Five fmol of the barcoded library were sequenced in a MinION (Oxford Nanopore Technologies) using a Flongle FLO-FLG001 flow cell (Oxford Nanopore Technologies). A total of 118 and 94 clones of CN PIP5Pase cells tet + (PIP5Pase expression) and tet - (PIP5Pase knockdown), respectively, were analyzed.

Preparation of DNA libraries and Oxford nanopore sequencing

DNA libraries were prepared using the ligation sequencing kit SQK-LSK110 (Oxford Nanopore Technologies), according to the manufacturer's instructions. Briefly, the fragmented nucleic acids were end-repaired and A-tailed using the NEBNext Ultra II End Repair and A-Tailing Module (New England Biolabs). The samples were cleaned with Totalpure NGS mag-bind (Omega-BioTek) at 0.85x ratio (beads to DNA volume), then ligated with nanopore barcode adapters. The product was subsequently used for PCR amplification with barcoding primers (Oxford Nanopore Technologies). The PCR product was cleaned with Totalpure NGS mag-bind (Omega-BioTek) at a 0.85x ratio (beads to DNA volume)

and ligated to motor proteins for DNA sequencing. The libraries were sequenced in a MinION Mk1C sequencer (Oxford Nanopore Technologies) using FLO-MIN106 flow cells (unless otherwise stated), and sequences were basecalled using the Guppy software (Oxford Nanopore Technologies). Sequencing information is available in Table S3 and fastq data is available in the Sequence Read Archive (SRA) with the BioProject identification PRJNA934938.

Computational analysis of RNA-seq and ChIP-seq

RNA-seq or ChIP-seq fastq data from nanopore sequencing were mapped to *T. brucei* 427-2018 reference genome using minimap2 (<https://github.com/lh3/minimap2>) and the alignment data were processed with SAMtools (<https://github.com/samtools/samtools>). Reads with a nanopore sequencing Q-score > 7 were used for analysis, and the mean Q-score was 12. RNA-seq mapped reads were quantified using featureCounts from package Subread (<https://bioconductor.org/packages/release/bioc/html/Rsubread.html>) and used for differential expression analysis using EgdeR (<https://bioconductor.org/packages/release/bioc/html/edgeR.html>). Alignments were filtered to remove supplementary alignments using samtools flags. Because RNA-seq reads were detected mapping to subtelomeric regions in cells expressing Mut PIP5Pase, differential expression analysis was also performed with alignments filtered for primary reads with a stringent mapping probability of 99.9% (mapQ 30) to eliminate potential multiple mapping reads. Read counts were obtained with featureCounts counting primary alignments only and processed using EgdeR. For ChIP-seq, aligned reads mapped with minimap2 were processed with deepTools for coverage analysis using bamCoverage and enrichment analysis using bamCompare (<https://deeptools.readthedocs.io/en/develop/>) comparing RAP1-HA ChIP vs Input. Peak calling and statistical analysis were performed for broad peaks with Model-based Analysis of ChIP-Seq MACS3 (<https://github.com/macs3-project/MACS>), and data were visualized using the integrated genomics viewer tool (Broad Institute). To identify if RAP1-HA was mapping specifically to silent vs active ESs, mapped reads were filtered to remove supplementary and secondary alignments, i.e., only primary alignments were considered for the analysis with a minimum mapping probability of 99% (mapQ 20). This stringent analysis removes reads aligning to multiple regions of the genome including reads mapping to multiple ESs, i.e., it retains reads aligning to specific regions of the ESs. Filtered reads were processed as described above using deepTools and MACS3 analysis.

Quantification of PI(3,4,5)P3

T. brucei BFs PIP5Pase CN cell lines exclusively expressing V5-tagged PIP5Pase WT or mutant D360A/N362A were grown in 100 mL HMI-9 media supplemented with 10% FBS, 2 µg/mL of G418, 2.5 µg/mL of phleomycin, and grown for 24 h in the absence of tet, which results in the exclusive expression of WT or Mut PIP5Pase. A total of 1.0×10^8 cells were used for PI(3,4,5)P3 quantification using Echelon's PIP3 Mass ELISA Kit (Echelon Biosciences), according to the manufacturer's instructions. Briefly, the cells were centrifuged at 2,000 xg at RT for 5 min, washed in PBS 6mM Glucose, and the supernatant was discarded. The cell pellets were resuspended in 10 mL of ice-cold 0.5 M Trichloroacetic Acid (TCA), incubated on ice for 5 min, then centrifuged at 1,000 xg for 7 min at 4°C. The supernatant was discarded, and the pellets were washed twice using 3 mL of 5% TCA/1 mM EDTA per wash at RT. Neutral lipids were extracted by adding 3 mL of MeOH: CHCl₃ (2:1) to the pellets and

vortexed for 10 min at RT, followed by centrifugation at 1,000 xg for 5 min, and the supernatant discarded. This step was repeated once more to remove neutral lipids. 2.25 mL of MeOH:CHCl₃:HCl (80:40:1) was added to the pellets and vortexed for 25 min at RT, then centrifuged at 1,000 xg for 5 min to extract the acidic lipids. The supernatants were transferred to new 15 mL centrifuge tubes. 0.75 mL CHCl₃ and 1.35 mL 0.1 N HCl were added to the supernatants, vortexed for 30 seconds, then centrifuged at 1,000 xg for 5 min to separate the organic and aqueous phases. 1.5 mL of the organic (lower) phase was transferred to new 2 mL vials and vacuum dried using a SpeedVac (Thermo Scientific) at RT. The dried lipids were stored at -20°C until used. To quantify PI(3,4,5)P₃ interacting with RAP1-HA, 300 mL of *T. brucei* BFs CN PIP5Pase expressing endogenously HA-tagged RAP1 and exclusively expressing V5-tagged PIP5Pase WT or mutant D360A/N362A were grown for 24h in absence of tet, which results in the exclusive expression of WT or mutant PIP5Pase, in HMI-9 media supplemented with 10% FBS, 2 µg/mL of G418, 2.5 µg/mL of phleomycin, 0.1 µg/mL of puromycin, and 25 µg/mL of nourseothricin. A total of 3x10⁸ cells (PIP5Pase WT and Mut) were centrifuged at 2,000 xg at RT for 5 min, washed in 20 mL of PBS 6 mM glucose and then lysed in 5 mL of *T. brucei* cell lysis buffer (50 mM Tris, 150 mM NaCl, 2X protein inhibitor cocktail, 0.1% NP-40, and 1% Triton-X100), rotating at 4°C for 30 min. Lysates were centrifuged at 15,000 xg, 4°C for 30 min, and the cleared lysate was transferred to a new 15 mL falcon tube. 2% (100 µL) of the cleared lysate was collected for Western blot of HA-tagged RAP1 (input). The remaining cleared lysate was used for RAP1-HA immunoprecipitation with anti-HA monoclonal antibodies (ABClonal). 20 µg of anti-HA monoclonal antibodies crosslinked to protein G MicroBeads (GE Healthcare) were added to the cleared lysate and incubated overnight at 4 °C. Immunoprecipitated samples on beads were washed five times in wash buffer (50 mM Tris, 150 mM NaCl, 2X protein inhibitor cocktail, 0.1% NP-40). An aliquote corresponding to 20% of the beads-bound samples was collected and eluted in 6M Urea/100 mM Glycine pH 2.9 for Western blot analysis of immunoprecipitated RAP1-HA protein. The remaining samples on the beads (80%) were used for acidic lipids extraction, as indicated above. The dried lipids were resuspended in PBS-T 0.25% Protein Stabilizer (PBS-T 0.25% PS), and PI(3,4,5)P₃ content was measured using Echelon's PIP₃ Mass ELISA Kit (Echelon Biosciences), according to the manufacturer's instructions.

Data presentation and statistical analysis

Data are shown as means ± SEM from at least three biological replicates. Comparisons among groups were made by a two-tailed t-test using GraphPad Prism. P-values < 0.05 with a confidence interval of 95% were considered statistically significant. Graphs were prepared using Prism (GraphPad Software, Inc.), MATLAB (Mathworks), or Integrated Genome Viewer (Broad Institute).

556 References

- 557 1. I. Cestari, K. Stuart, Transcriptional Regulation of Telomeric Expression Sites and Antigenic Variation in
558 Trypanosomes. *Curr Genomics* **19**, 119-132 (2018).
- 559 2. M. Navarro, K. Gull, A pol I transcriptional body associated with VSG mono-allelic expression in
560 Trypanosoma brucei. *Nature* **414**, 759-763 (2001).
- 561 3. D. Horn, G. A. Cross, A developmentally regulated position effect at a telomeric locus in Trypanosoma
562 brucei. *Cell* **83**, 555-561 (1995).
- 563 4. G. Rudenko, P. A. Blundell, A. Dirks-Mulder, R. Kieft, P. Borst, A ribosomal DNA promoter replacing the
564 promoter of a telomeric VSG gene expression site can be efficiently switched on and off in T. brucei. *Cell*
565 **83**, 547-553 (1995).
- 566 5. X. Yang, L. M. Figueiredo, A. Espinal, E. Okubo, B. Li, RAP1 is essential for silencing telomeric variant
567 surface glycoprotein genes in Trypanosoma brucei. *Cell* **137**, 99-109 (2009).
- 568 6. J. A. Baur, Y. Zou, J. W. Shay, W. E. Wright, Telomere position effect in human cells. *Science* **292**, 2075-
569 2077 (2001).
- 570 7. L. R. Myler *et al.*, The evolution of metazoan shelterin. *Genes Dev* **35**, 1625-1641 (2021).
- 571 8. G. Kyrion, K. Liu, C. Liu, A. J. Lustig, RAP1 and telomere structure regulate telomere position effects in
572 Saccharomyces cerevisiae. *Genes Dev* **7**, 1146-1159 (1993).
- 573 9. T. de Lange, Shelterin: the protein complex that shapes and safeguards human telomeres. *Genes Dev* **19**,
574 2100-2110 (2005).
- 575 10. L. Lototska *et al.*, Human RAP1 specifically protects telomeres of senescent cells from DNA damage.
576 *EMBO Rep* **21**, e49076 (2020).
- 577 11. J. M. Platt *et al.*, Rap1 relocalization contributes to the chromatin-mediated gene expression profile and
578 pace of cell senescence. *Genes Dev* **27**, 1406-1420 (2013).
- 579 12. L. M. Figueiredo, G. A. Cross, Nucleosomes are depleted at the VSG expression site transcribed by RNA
580 polymerase I in African trypanosomes. *Eukaryot Cell* **9**, 148-154 (2010).
- 581 13. L. S. M. Muller *et al.*, Genome organization and DNA accessibility control antigenic variation in
582 trypanosomes. *Nature* **563**, 121-125 (2018).
- 583 14. L. M. Figueiredo, C. J. Janzen, G. A. Cross, A histone methyltransferase modulates antigenic variation in
584 African trypanosomes. *PLoS Biol* **6**, e161 (2008).
- 585 15. D. Schulz *et al.*, Bromodomain Proteins Contribute to Maintenance of Bloodstream Form Stage Identity
586 in the African Trypanosome. *PLoS Biol* **13**, e1002316 (2015).
- 587 16. L. Glover, S. Hutchinson, S. Alsford, D. Horn, VEX1 controls the allelic exclusion required for antigenic
588 variation in trypanosomes. *Proc Natl Acad Sci U S A* **113**, 7225-7230 (2016).
- 589 17. J. Faria *et al.*, Monoallelic expression and epigenetic inheritance sustained by a Trypanosoma brucei
590 variant surface glycoprotein exclusion complex. *Nat Commun* **10**, 3023 (2019).
- 591 18. K. W. Deitsch, S. A. Lukehart, J. R. Stringer, Common strategies for antigenic variation by bacterial, fungal
592 and protozoan pathogens. *Nat Rev Microbiol* **7**, 493-503 (2009).
- 593 19. C. E. Boothroyd *et al.*, A yeast-endonuclease-generated DNA break induces antigenic switching in
594 Trypanosoma brucei. *Nature* **459**, 278-281 (2009).
- 595 20. E. Briggs, K. Crouch, L. Lemgruber, C. Lapsley, R. McCulloch, Ribonuclease H1-targeted R-loops in surface
596 antigen gene expression sites can direct trypanosome immune evasion. *PLoS Genet* **14**, e1007729 (2018).

- 597 21. M. S. da Silva, G. A. Hovel-Miner, E. M. Briggs, M. C. Elias, R. McCulloch, Evaluation of mechanisms that
598 may generate DNA lesions triggering antigenic variation in African trypanosomes. *PLoS Pathog* **14**,
599 e1007321 (2018).
- 600 22. R. McCulloch, J. D. Barry, A role for RAD51 and homologous recombination in *Trypanosoma brucei*
601 antigenic variation. *Genes Dev* **13**, 2875-2888 (1999).
- 602 23. I. Cestari, K. Stuart, Inositol phosphate pathway controls transcription of telomeric expression sites in
603 trypanosomes. *Proc Natl Acad Sci U S A* **112**, E2803-2812 (2015).
- 604 24. I. Cestari, H. McLeland-Wieser, K. Stuart, Nuclear Phosphatidylinositol 5-Phosphatase Is Essential for
605 Allelic Exclusion of Variant Surface Glycoprotein Genes in Trypanosomes. *Mol Cell Biol* **39** (2019).
- 606 25. I. Cestari, Identification of Inositol Phosphate or Phosphoinositide Interacting Proteins by Affinity
607 Chromatography Coupled to Western Blot or Mass Spectrometry. *J Vis Exp* 10.3791/59865 (2019).
- 608 26. S. O. Obado, C. Bot, D. Nilsson, B. Andersson, J. M. Kelly, Repetitive DNA is associated with centromeric
609 domains in *Trypanosoma brucei* but not *Trypanosoma cruzi*. *Genome Biol* **8**, R37 (2007).
- 610 27. B. Akiyoshi, K. Gull, Discovery of unconventional kinetochores in kinetoplastids. *Cell* **156**, 1247-1258
611 (2014).
- 612 28. M. Afrin, H. Kishmiri, R. Sandhu, M. A. G. Rabbani, B. Li, *Trypanosoma brucei* RAP1 Has Essential
613 Functional Domains That Are Required for Different Protein Interactions. *mSphere* **5** (2020).
- 614 29. M. Afrin *et al.*, TbRAP1 has an unusual duplex DNA binding activity required for its telomere localization
615 and VSG silencing. *Sci Adv* **6** (2020).
- 616 30. N. Kumar, P. Zhao, A. Tomar, C. A. Galea, S. Khurana, Association of villin with phosphatidylinositol 4,5-
617 bisphosphate regulates the actin cytoskeleton. *J Biol Chem* **279**, 3096-3110 (2004).
- 618 31. T. K. Chiu *et al.*, High-resolution x-ray crystal structures of the villin headpiece subdomain, an ultrafast
619 folding protein. *Proc Natl Acad Sci U S A* **102**, 7517-7522 (2005).
- 620 32. J. Meng, C. J. McKnight, Heterogeneity and dynamics in villin headpiece crystal structures. *Acta*
621 *Crystallogr D Biol Crystallogr* **65**, 470-476 (2009).
- 622 33. V. Nanavaty, R. Sandhu, S. E. Jehi, U. M. Pandya, B. Li, *Trypanosoma brucei* RAP1 maintains telomere and
623 subtelomere integrity by suppressing TERRA and telomeric RNA:DNA hybrids. *Nucleic Acids Res* **45**, 5785-
624 5796 (2017).
- 625 34. K. N. DuBois *et al.*, NUP-1 Is a large coiled-coil nucleoskeletal protein in trypanosomes with lamin-like
626 functions. *PLoS Biol* **10**, e1001287 (2012).
- 627 35. K. L. Martin, T. K. Smith, Phosphatidylinositol synthesis is essential in bloodstream form *Trypanosoma*
628 *brucei*. *Biochem J* **396**, 287-295 (2006).
- 629 36. Y. J. Kim, M. L. Guzman-Hernandez, T. Balla, A highly dynamic ER-derived phosphatidylinositol-
630 synthesizing organelle supplies phosphoinositides to cellular membranes. *Dev Cell* **21**, 813-824 (2011).
- 631 37. A. K. Gaurav *et al.*, The RRM-mediated RNA binding activity in *T. brucei* RAP1 is essential for VSG
632 monoallelic expression. *Nat Commun* **14**, 1576 (2023).
- 633 38. L. Lopez-Escobar *et al.*, Stage-specific transcription activator ESB1 regulates monoallelic antigen
634 expression in *Trypanosoma brucei*. *Nat Microbiol* **7**, 1280-1290 (2022).
- 635 39. J. Faria *et al.*, Spatial integration of transcription and splicing in a dedicated compartment sustains
636 monogenic antigen expression in African trypanosomes. *Nat Microbiol* **6**, 289-300 (2021).
- 637 40. J. Budzak, R. Jones, C. Tschudi, N. G. Kolev, G. Rudenko, An assembly of nuclear bodies associates with
638 the active VSG expression site in African trypanosomes. *Nat Commun* **13**, 101 (2022).

- 639 41. M. R. Mugnier, G. A. Cross, F. N. Papavasiliou, The in vivo dynamics of antigenic variation in *Trypanosoma*
640 *brucei*. *Science* **347**, 1470-1473 (2015).

641

642

643 **Acknowledgments**

644 This research was enabled in part by computational resources provided by Calcul Quebec
645 (<https://www.calculquebec.ca/en/>) and the Digital Research Alliance of Canada (alliancecan.ca).

646 **Funding:**

647 Canadian Institutes of Health Research grant CIHR PJT-175222 (IC)
648 The Natural Sciences and Engineering Research Council of Canada grant RGPIN-2019-05271
649 (IC)
650 Fonds de Recherche du Québec - Nature et technologie grant 2021-NC-288072 (IC)
651 Canada Foundation for Innovation grant JELF 258389 (IC)
652 McGill University fund 130251 (IC)
653 Islamic Development Bank Scholarship 600042744 (AOT)
654 FRQNT-Ukraine postdoctoral fellowship BUKX:2022-2023 337989 (OK)
655 The Natural Sciences and Engineering Research Council of Canada CGS M fellowship (ML)

656 **Author contributions:**

657 Conceptualization: IC
658 Methodology: IC, AOT, TI, TS
659 Investigation: IC, AOT, RR, TI, ML, TS, OK
660 Visualization: IC, TS, AOT, ML
661 Funding acquisition: IC
662 Project administration: IC
663 Supervision: IC
664 Writing – original draft: IC
665 Writing – review & editing: IC, AOT, RR, TI, ML, TS, OK

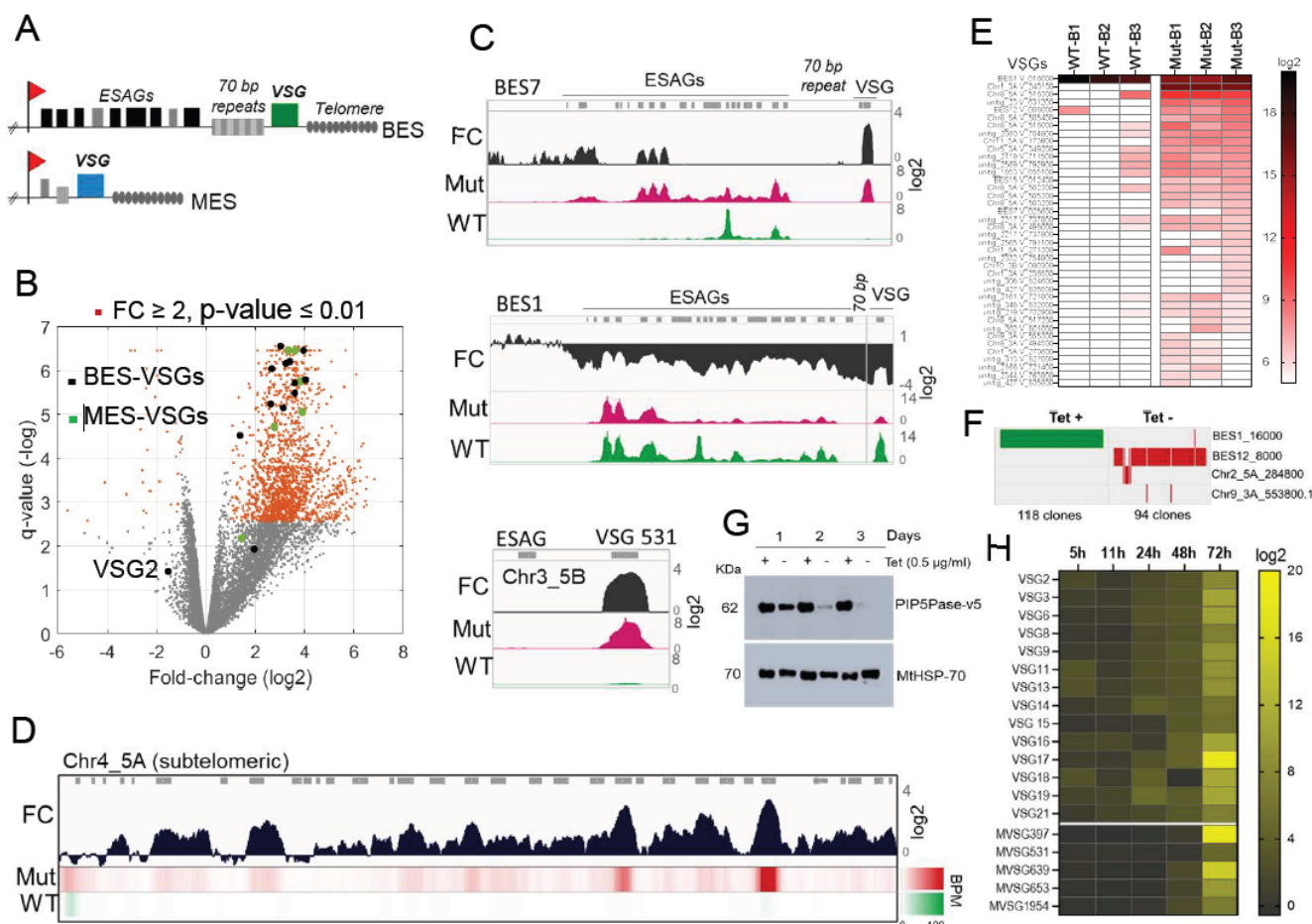
666 **Competing interests:** Authors declare that they have no competing interests.

667 **Data and materials availability:** RNA-seq and ChIP-seq sequencing data is available in the
668 Sequence Read Archive (SRA) with the BioProject identification PRJNA934938.

669 **Supplementary Materials**

670 Figs. S1 to S7
671 Tables S1 to S3
672 Data S1 to S2
673

Figures and Figure legends



675

Fig 1. PIP5Pase activity is essential for VSG gene silencing and switching. A) Diagram of bloodstream-form ESs (BES, top) and metacyclic-form ESs (MES, bottom). B) RNA-seq analysis of *T. brucei* bloodstream forms comparing 24h exclusive expression of Mut to WT PIP5Pase. FC, fold-change. C-D) RNA-seq read coverage and FC (Mut vs WT) of silent BES7 (C, top), the active BES1 (C, middle), a silent MESs (C, bottom), and chromosome 4 subteloemere (D). Heat-map in D shows RNA-seq bins per million (BPM) reads. Gray rectangles represent genes. A 99.9% reads mapping probability to the genome (mapQ>30) retained alignments to subtelomeric regions. E) VSG-seq analysis of *T. brucei* bloodstream forms after temporary (24h) exclusive expression of Mut PIP5Pase, and re-expression of WT PIP5Pase (60h). B1-B3, biological replicates. The color shows normalized read counts per million. A 3'-end conserved VSG sequence was used to capture VSG mRNAs (41). F) VSG-seq analysis of isolated clones after PIP5Pase temporary knockdown (tet -, 24h) followed by its re-expression (Tet +) and cloning for 5-7 days. Clones of non-knockdown (tet +) cells were analyzed as controls. G) Western blot of V5-tagged PIP5Pase knockdown in *T. brucei* procyclic forms. The membrane was stripped and reprobed with anti-mitochondrial heat shock protein 70 (MthSP70). H) Expression analysis of ES VSG genes after knockdown of PIP5Pase in procyclic forms. Data are the result of three biological replicates.

691

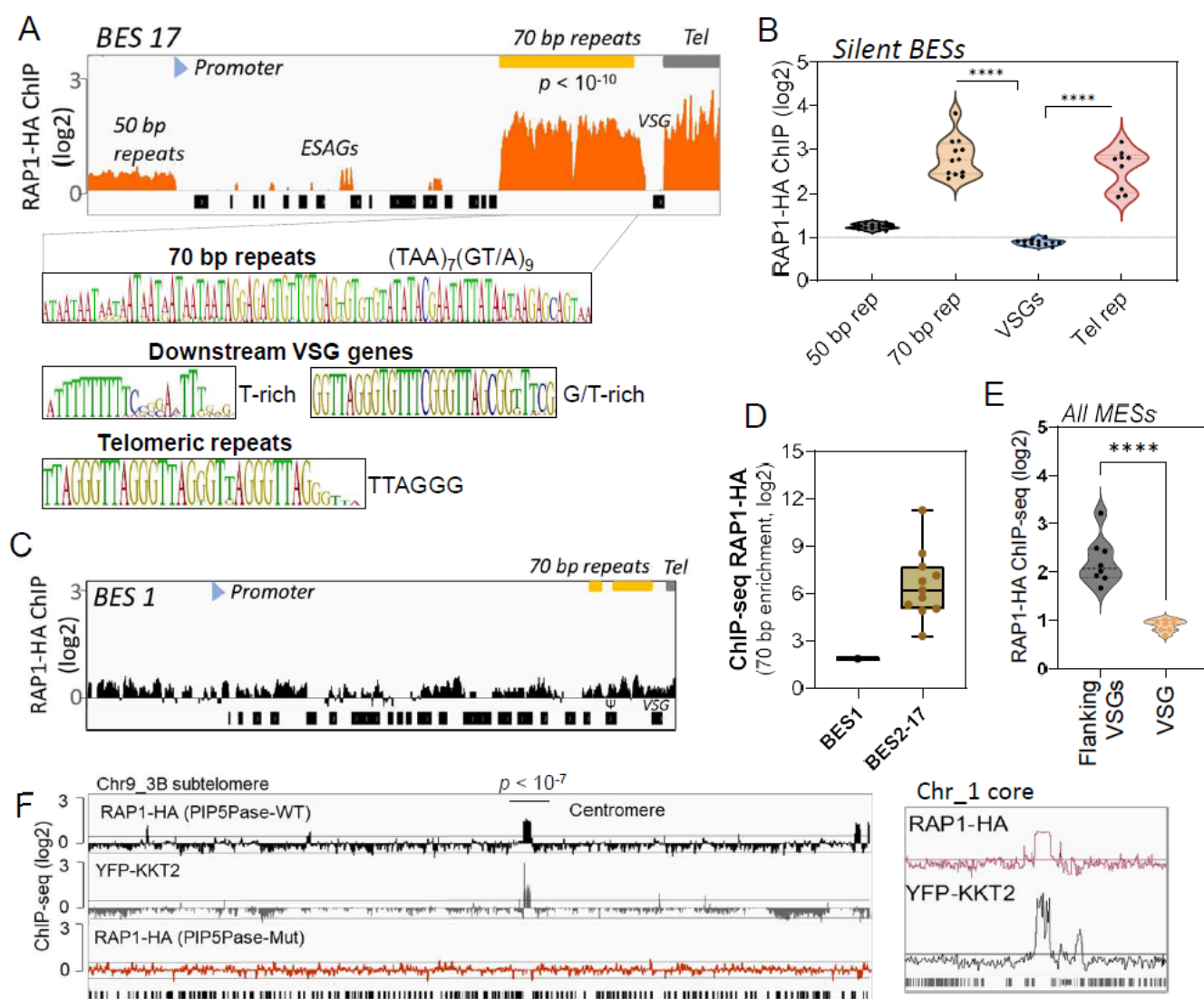


Fig 2. ChIP-seq analysis of RAP1-HA in *T. brucei*. A) RAP1-HA binding sites on the silent BES17. Below, sequence bias of bound regions. B) RAP1-HA binding to selected regions in silent BES sequences. Each dot represents the mean of a silent BES. C) RAP1-HA enrichment to the active BES1. Reads were filtered for over 99% mapping probability (primary reads only, mapQ>20). D) Comparison of RAP1-HA binding to 70 bp in silent and active ESs. E) RAP1-HA enrichment over all MESs. F) RAP1-HA binding to subtelomere 3B of chromosome (Chr) 9 (left) or chromosome 1 core (right). Yellow fluorescent protein (YFP)-tagged KKT2 protein ChIP-seq from (27) is shown. RAP1-HA ChIP-seq in cells expressing Mut PIP5Pase is shown below. p -values (p) were calculated using Model-based Analysis of ChIP-Seq (MACS) from three biological replicates. All data show ChIP vs Input analysis. See Table S1 and Data S2 for detailed statistics. ****, p -value < 0.0001.

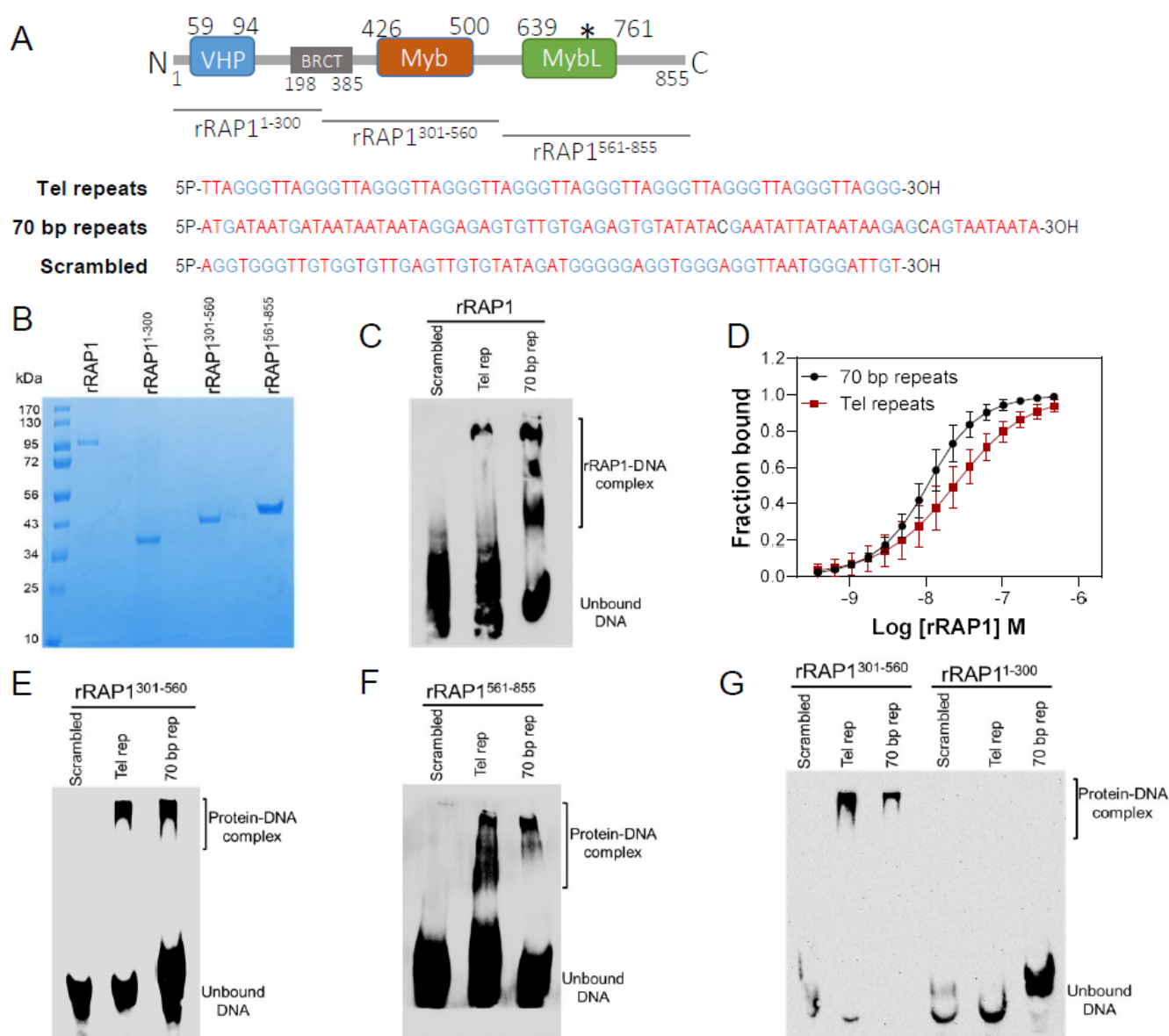


Fig 3. rRAP1 binds to telomeric and 70 bp repeats via its Myb and MybL domain. A) Top, RAP1 diagram shows VHP, BRCT, Myb and MybL domains. Numbers indicate residue positions; asterisk, nuclear targeting sequence. Bottom, telomeric (10 repeats), 70 bp (one repeat), or scrambled (generated from telomeric repeats) sequences used in binding assays. B) His-tagged rRAP1, rRAP1¹⁻³⁰⁰, rRAP³⁰¹⁻⁵⁶⁰, and rRAP1⁵⁶¹⁻⁸⁵⁵ resolved in 10% SDS/PAGE and Coomassie-stained. C) EMSA of His-tagged rRAP1 with biotinylated telomeric repeats (Tel rep), 70 repeats (70 bp rep), or scrambled sequences resolved in 6% native/PAGE and developed with Streptavidin-HRP. D) MST binding kinetics of rRAP1 with Cy5-labelled telomeric repeats or 70 bp repeats. Data shown are the mean \pm SDM of four biological replicates. E-G) EMSA of rRAP1³⁰¹⁻⁵⁶⁰ (E), rRAP1⁵⁶¹⁻⁸⁵⁵ (F), or rRAP1¹⁻³⁰⁰ (G) with telomeric, 70 bp repeats, or scrambled sequences resolved in 6% native/PAGE. rRAP1³⁰¹⁻⁵⁶⁰ were used as a positive control in G.

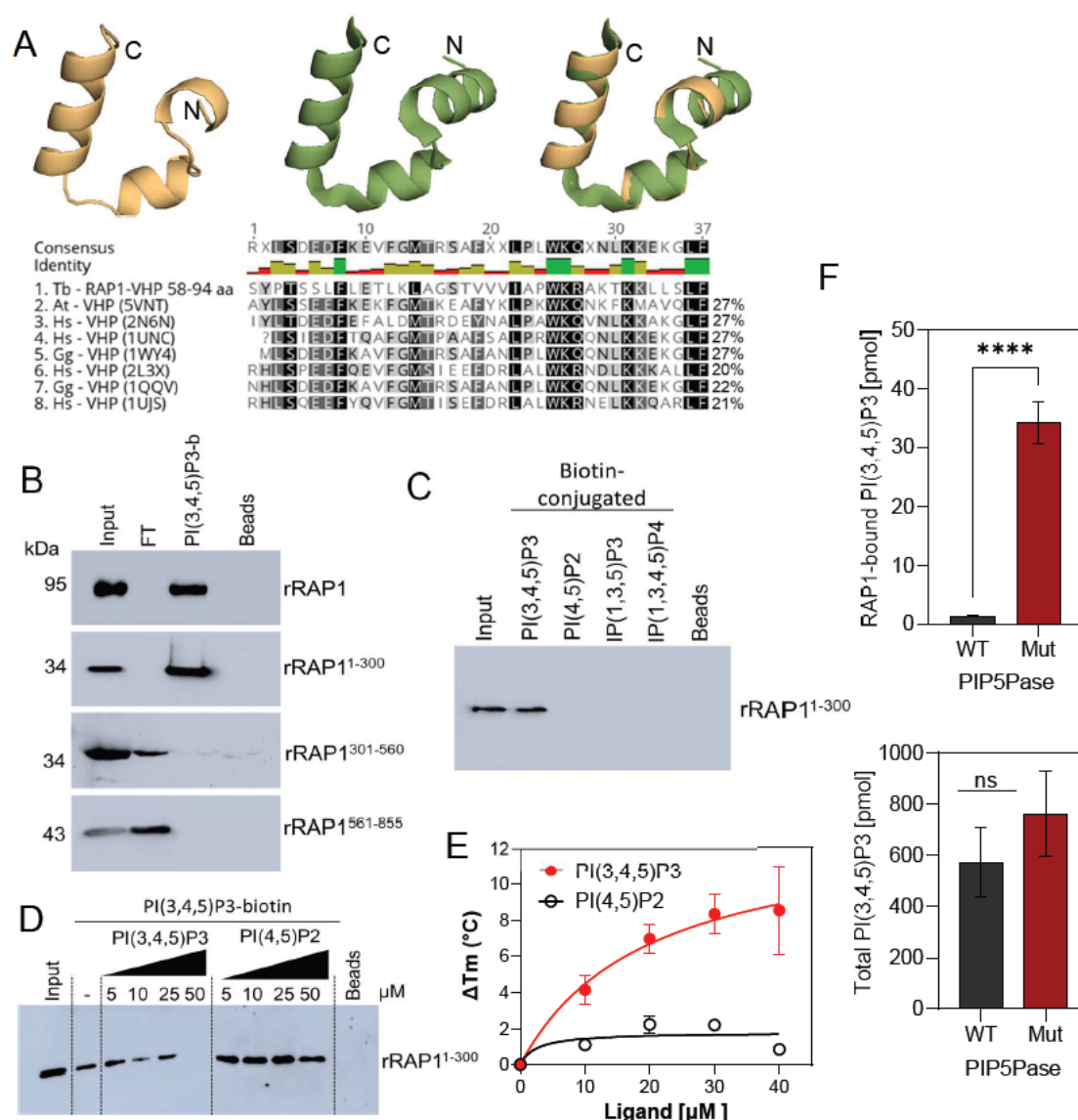


Fig 4. rRAP1 binds to PI(3,4,5)P3 through its N-terminus. A) Modeling and alignment of RAP1 VHP domain. *Left*, RAP1 modeled structure; *middle*, VHP domain structure of human supervillin protein (PDB accession number 2K6N); and *right*, superposition of *T. brucei* RAP1 modeled VHP and human supervillin VHP domains. Alignment of *T. brucei* RAP1 VHP with human (Hs), *Arabidopsis thaliana* (At), and *Gallus gallus* (Gg) VHP domains from Villin proteins. PDB accession numbers are indicated in parenthesis. % of aa identity to *T. brucei* sequence are shown. B) Binding assays with rRAP1, rRAP1¹⁻³⁰⁰, rRAP1³⁰¹⁻⁵⁶⁰, or rRAP1⁵⁶¹⁻⁸⁵⁵ and PI(3,4,5)P3-biotin. Beads, Streptavidin-beads; FT, flow-through. Proteins were resolved in 10% SDS/PAGE and Western developed with α -His mAbs. C) Binding of His-tagged rRAP1¹⁻³⁰⁰ to biotinylated phosphoinositides or IPs. D) Binding of rRAP1¹⁻³⁰⁰ to PI(3,4,5)P3-biotin in presence of unlabelled PI(3,4,5)P3 or PI(4,5)P2. For C and D, proteins were analyzed as in B. E) Binding kinetics of rRAP1 with unlabelled PI(3,4,5)P3 or PI(4,5)P2. ΔT_m , change in melting temperature. Data show the mean \pm SDM of three biological replicates. F) Quantification of RAP1-bound PI(3,4,5)P3 (top) or total cellular PI(3,4,5)P3 (bottom) levels in *T. brucei* exclusively expressing WT or Mut PIP5Pase. Data show the mean \pm SDM of four biological replicates. ****, p -value < 0.0001.

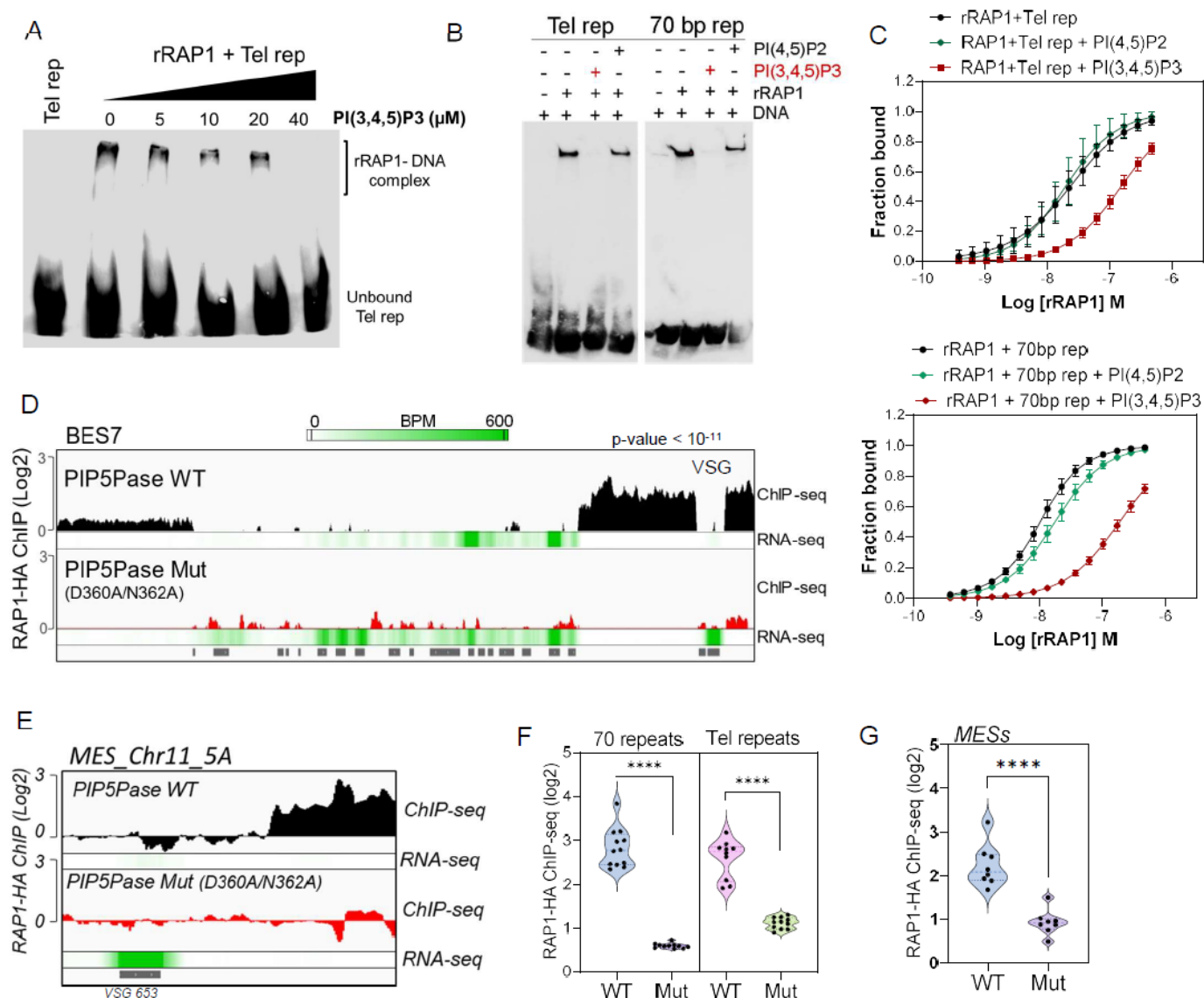


Fig 5. PIP5Pase controls rRAP1 binding to telomeric ESs via PI(3,4,5)P3. A) EMSA of rRAP1 with biotinylated telomeric repeats and increasing concentrations of PI(3,4,5)P3. B) EMSA of rRAP1 with biotinylated telomeric repeats (left) or 70 bp repeats (right) and 30 μM of PI(3,4,5)P3 or PI(4,5)P2. For A-B, samples were resolved in 6% native/PAGE, transferred to nylon membranes, and developed with streptavidin-HRP. C) MST binding kinetics of rRAP1 with Cy5-labelled telomeric repeats (top) or 70 bp repeats (bottom) with 30 μM of PI(3,4,5)P3 or PI(4,5)P2. Data show the mean ± SDM of four biological replicates. D-E) ChIP-seq of RAP1-HA binding to BES7 (D) or (MES_Ch11_5A) from cells that exclusively express WT or Mut PIP5Pase for 24h. RNA-seq comparing exclusive expression of Mut vs WT PIP5Pase for 24h is shown. F-G) Violin plots show RAP1-HA mean enrichment over 70 bp or telomeric repeats from all silent BESs (F) or MESs (G). Each dot represents an ES. BPM, bin per million. ChIP-seq and RNA-seq were performed in three biological replicates. ****, $p < 0.0001$.

Table 1. Binding kinetics of rRAP1 to telomeric repeats, 70 bp repeats, and phosphoinositides.
Data show the mean ± standard deviation of the mean (SDM).

Interactions		Kd [M] ± SDM
rRAP1 + Telomeric repeats		$24.1 \times 10^{-9} \pm 2.0 \times 10^{-9}$
rRAP1 + 70 bp repeats		$10.0 \times 10^{-9} \pm 0.33 \times 10^{-9}$
rRAP1 + PI(3,4,5)P3		$19.7 \times 10^{-6} \pm 2.8 \times 10^{-6}$
rRAP1 + PI(4,5)P2		No binding
rRAP1 + Telomeric repeats + PI(3,4,5)P3		$154.6 \times 10^{-9} \pm 14.2 \times 10^{-9}$
rRAP1 + Telomeric repeats + PI(4,5)P2		$19.4 \times 10^{-9} \pm 1.5 \times 10^{-9}$
rRAP1 + 70 bp repeats + PI(3,4,5)P3		$187.7 \times 10^{-9} \pm 29.9 \times 10^{-9}$
rRAP1 + 70 bp repeats + PI(4,5)P2		$17.5 \times 10^{-8} \pm 0.9 \times 10^{-9}$